# UC Berkeley
## UC Berkeley Previously Published Works

**Title**

Heterologous boost with mRNA vaccines against SARS-CoV-2 Delta/Omicron variants following an inactivated whole-virus vaccine.

**Permalink**

https://escholarship.org/uc/item/8zc610wh

**Authors**

Lu, Changrui

Zhang, Yuntao

Liu, Xiaohu

et al.

**Publication Date**

2023-04-01

**DOI**

10.1016/j.antiviral.2023.105556

Peer reviewed

Check for updates

# Heterologous boost with mRNA vaccines against SARS-CoV-2 Delta/Omicron variants following an inactivated whole-virus vaccine

Changrui Lu [a,1], Yuntao Zhang [b,1], Xiaohu Liu [c], Fujun Hou [c], Rujie Cai [a], Zhibin Yu [c], Fei Liu [a], Guohuan Yang [a], Jun Ding [c], Jiang Xu [c], Xianwu Hua [c], Xinhua Cheng [a], Xinping Pan [a], Lianxiao Liu [a], Kang Lin [a], Zejun Wang [d], Xinguo Li [d], Jia Lu [d], Qiu Zhang [d], Yuwei Li [d], Chunxia Hu [d], Huifen Fan [d], Xiaoke Liu [d], Hui Wang [d], Rui Jia [b], Fangjingwei Xu [b], Xuewei Wang [b], Hongwei Huang [a,c], Ronghua Zhao [a,c], Jing Li [e], Hang Cheng [e], William Jia [a,c,**], Xiaoming Yang [b,*]

[a] China National Biological Group-Virogin Biotech (Shanghai) Ltd (CNBG-Virogin), China
[b] China National Biotec Group (CNBG), China
[c] Virogin Biotech (Shanghai) Ltd (Virogin), China
[d] Wuhan Institute of Biological Products Co., LTD (WIBP), China
[e] Shuimu BioSciences Ltd, China

## A B S T R A C T

The coronavirus SARS-CoV-2 has mutated quickly and caused significant global damage. This study characterizes two mRNA vaccines ZSVG-02 (Delta) and ZSVG-02-O (Omicron BA.1), and associating heterologous prime-boost strategy following the prime of a most widely administrated inactivated whole-virus vaccine (BBIBP-CorV). The ZSVG-02-O induces neutralizing antibodies that effectively cross-react with Omicron subvariants. In naïve animals, ZSVG-02 or ZSVG-02-O induce humoral responses skewed to the vaccine's targeting strains, but cellular immune responses cross-react to all variants of concern (VOCs) tested. Following heterologous prime-boost regimes, animals present comparable neutralizing antibody levels and superior protection against Delta and Omicron BA.1variants. Single-boost only generated ancestral and omicron dual-responsive antibodies, probably by "recall" and "reshape" the prime immunity. New Omicron-specific antibody populations, however, appeared only following the second boost with ZSVG-02-O. Overall, our results support a heterologous boost with ZSVG-02-O, providing the best protection against current VOCs in inactivated virus vaccine–primed populations.

## 1. Introduction

The coronavirus SARS-CoV-2 and its developing variants spread quickly across borders, causing hundreds of millions of infected cases and several millions of deaths worldwide as of 2021 (Su et al., 2020).

Currently our most potent countermeasure, COVID-19 vaccines have a number of platforms including inactivated whole-virus (Ella et al., 2021), subunit vaccines (Heath et al., 2021), lipid nanoparticles (LNP) mRNA (Baden et al., 2021; Polack et al., 2020), adenoviral vectors expressing viral Spike protein (Watanabe et al., 2021) and various recombinant S protein vaccines and DNA vaccines (Yadav et al., 2020).

While mRNA vaccines induce higher antibody titers, inactivated whole-virus vaccines have had many years of manufacture and clinical experience. Moreover, inactivated whole-virus vaccines may induce a broader breadth of immunity, specifically for viral structure proteins other than just the S protein.

While the current vaccines have proven very effective against the original COVID-19 (SARS-CoV-2 ancestral strain), emerging new variants of concern (VOCs) have quickly reduced their efficacy due to mutations that escape antibody neutralization (Flemming, 2022; Tada et al., 2021; Wu et al., 2021; Qu et al., 2022). Recent variants, including BA.1 (Thakur and Ratho, 2021), BA.2 (Chen and Wei, 2022), BA.3

(B.1.1.529.3) (Desingu et al., 2022) and BA4/5 (Tegally et al., 2022), can resist neutralizing antibodies induced by either virus infection or currently approved COVID-19 vaccines (Weigang et al., 2021; Pegu et al., 2021; Andreano et al., 2021; Liu et al., 2021; Yamasoba et al., 2022). While booster shots of BNT162b2 or mRNA-1273 effectively prevent severe symptoms, breakthrough infections with the Omicron variants in people have been widely reported (Kuhlmann et al., 2022). Therefore, updated booster vaccines and associated immunization schemes against new VOCs remain urgently necessary.

Given the advantages of inactivated whole-virus vaccines in immunity breadth and a vast population primed with them worldwide, an effective boost strategy against current Omicron variants requires extensive studies (Mallapaty, 2021). Recent studies show that two doses of the inactivated whole-virus vaccine, followed by one mRNA (BNT162b2 or mRNA-1273) as the booster, can prominently increase the humoral and cellular immune responses to COVID variants, but less effective for Omicron variant (van der Straten et al., 2022) (Zuo et al., 2022). Other studies reported that a viral vector vaccine primer plus an mRNA booster exhibited a high level of cross-neutralizing activity for the ancestral, Beta, Delta, and Omicron strains (Stamatatos et al., 2021; Wang et al., 2022). Clinical studies of heterologous boost with mRNA and adenovirus vaccines against the ancestral SARS-CoV-2 following two doses of the BBIBP-CorV vaccine have also been conducted (Wang et al., 2020). While the heterologous boost vaccination was safe, the inhibition for omicron variant measured less than 70% by a surrogate neutralization test (Chansaenroj et al., 2022). Inactivated whole virus vaccines of ancestral SARS-CoV-2, such as Sinopharm (BBIBP-CorV) and Sinovac (CoronaVac), have reached worldwide popularity and helped to mitigate the pandemic in many countries, especially in less developed areas (Al Kaabi et al., 2022; Ophinni et al., 2020). It is important to demonstrate that a heterologous boosting with a mRNA vaccine designed for omicron variants following the above inactivated virus vaccine can be effective against Omicron variants and furthermore, can broaden the immunity for multiple variants of SARS-CoV-2.

Here we report two new SARS-CoV-2 mRNA vaccines, ZSVG-02 and ZSVG-02-O, against Delta B.1.617.2 variant and Omicron B.1.1.529.1 (BA.1 subvariant), respectively. Both induce high neutralizing antibody levels against the variants in mouse models. In addition, the ZSVG-02-O-induced neutralizing antibodies can cross react with Omicron subvariant BA.2 and BA.4/5, albeit with reduced activity. Serving as a boost to BBIBP-CorV (Wang et al., 2020), both vaccines induce additional

protection across all VOCs tested in an ACE2-expressing mouse model. Moreover, our results demonstrate that a heterologous boost strategy with ZSVG-02-O following BBIBP-CorV priming produces superior protective immunity over homologous boosts. The heterologous prime-boost strategy with BBIBP-CorV and ZSVG-02-O takes advantages of both the primer and booster vaccines that the mRNA vaccines targeting the new VOCs and also recalling a broad breadth of immunity against SARS-Cov-2 built by the previously primed BBIBP-CorV.

## 2. Results

### 2.1. ZSVG-02- and ZSVG-02-O-encode active spike proteins analysed with cryo-EM

In order to confirm structures of the Delta and Omicron Spike proteins expressed by ZSVG-02 and ZSVG-02-O vaccines, we first tested their expression in transfected cells. The mRNA-LNPs were prepared and characterized following a classic protocol (Figs. S1A–D). Naked or LNP-encapsulated, ZSVG-02 and ZSVG-02-O expressed their corresponding S protein in transfected HEK293 cells (Fig. 1A, S1E). Specifically, the LNP ensured nearly 100% transfection efficiency of both ZSVG-02 and ZSVG-02-O in cells, measured by flow cytometry using a labeled angiotensin-converting enzyme 2 (ACE2) protein (Fig. 1B). The resulting S-protein antigens expressed by the transfected cells can also bind to receptor-binding domain (RBD)-specific antibodies against other variants (Fig. S1F). Antibodies against RBD can completely displace ACE2 binding to the ZSVG-02 transfected cells, showing that it competes with ACE2 for Spike binding (Fig. S1G). Overall, our mRNA-LNP formulation ensure minimum immunogenicity shown by very low IFNα and TNF-α levels (Figs. S1H–I).

Next, we used cryogenic electron microscopy (Cryo-EM) and single particle analysis (SPA) methods to determine the 3D structures of S protein from the two variants. We determined the overall resolution of Delta Spike protein open state with 1 receptor-binding domain (RBD) up at 2.64 Å, 2 RBD up at 2.77 Å, and Omicron Spike protein open states with 1 RBD up at 3.02 Å, and 2 RBD up at 3.02 Å respectively (Fig. S1J-L). We have built the 3D models for all four cryo-EM maps that covered most domains (Fig. 1C). Our 3D Heterogeneous Refinement shows that amongst all 2D particles for the Delta Spike protein, 43.1% belongs to the 1up-2down conformation, while 40.4% belongs to the 2up-1down conformation. The Omicron Spike showed 10.9% 1up-2down
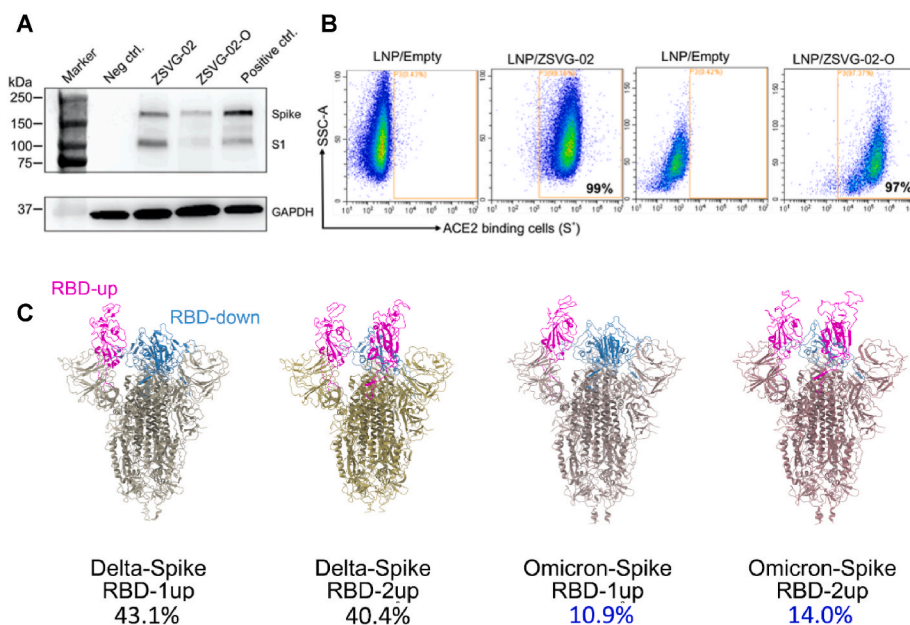


Fig. 1. Naked or LNP-encapsuled mRNA transfected to HEK293T/17 cells show specific spike protein expression. The 3D EM maps and 3D models for different Delta and Omicron Spike proteins produced from ZSVG-02 and ZSVG-02-O mRNA. (A). Detection of SARS-CoV-2 spike proteins expressed by naked mRNA of either ZSVG-02 or ZSVG-02-O in cells lysate via Western Blot. Cell lysates of mock (empty lipofectamine 3000) and pcDNA3.1(−) plasmid expressing S-protein transfections as negative and positive controls, respectively. n = 4, (B). Representative flow plots from 4 independent experiments showing the expression of LNP-encapsulated ZSVG-02 or ZSVG-02-O on cell surface by binding with 2.5 μg/mL ACE2 protein. The threshold was set according to the empty LNP transfected cells. (C) 3D models built from EM maps. Delta spike active state with 2 up RBD is colored with corn khaki. Omicron spike active state with 1 up RBD is colored with misty rose. Omicron spike active state with 2 up RBD is colored with misty pink. The up state RBD is highlighted with magenta. The down state RBD is highlighted with steel blue. Numbers underneath each model indicate the percentage of each conformation within total particles after 2D classification for Delta and Omicron respectively.

conformation and 14% 2up-1down conformation (Fig. 1C). Compared to the Delta Spike, the Omicron counterpart shows greater flexibility with more than 60% particles belonging to the "middle" RBD conformation, somewhere between up and down (data not shown). Fig. S1M shows the Fourier shell correlation (FSC) curves of 3D reconstruction models. The resolution value labeled near the FSC dash line indicates the FSC = 0.143 cutoff. Fig. S1N shows typical 2D particle images of Delta Spike (left) and Omicron Spike (right) proteins from ZSVG-02 and ZSVG-02-O. Fig. S1O shows the RMSD values of each model chain compared with the references model (PDB 7tpf, 7tph, 7wvn and 7wvo). The Omicron RBD domains show lowest resolution compared to Delta counterparts, indicating more structural dynamic.

### 2.2. ZSVG-02-O elicits strong humoral and cellular immune response against omicron subvariants

To determine the ability of the mRNA vaccines to induce neutralizing antibodies (nAbs) against current SARS-CoV-2 VOCs, BALB/c mice received two doses of ZSVG-02-O over either a two- or three-week interval (Fig. 2). The sera were collected 7 days following the second immunization to measure neutralizing antibodies against Omicron (BA.1) live virus. Fig. 2A shows that ZSVG-02-O induces high levels of anti-Omicron BA.1 neutralizing antibodies, while levels against ancestral strain and Delta strains are moderate for the middle and high doses and barely detectable for the lowest dose. This result proves variant specificity of ZSVG-02-O-induced immune response directly targeting the Omicron variant. Parallel experiments with the Delta-specific vaccine ZSVG-02 showed similar results with the most neutralizing antibodies against Delta followed by that for the ancestral strain. However, the antibody levels for Omicron variant BA.1 drop by 60- and 16-fold compared to Delta for the two doses tested (Fig. S2). In addition, we also tested ZSVG-02-O against Omicron BA.4.6, BF.7, BQ.1.1 and XBB pseudoviruses and the results show that despite decreased efficacy, ZSVG-02-O still elicit adequate nAb levels (Fig. S3).

To investigate ZSVG-02-O-induced humoral immunity across the current Omicron subvariants, the sera of ZSVG-02-O-vaccinated animals were collected fourteen or twenty-one days following the second dose and nAb levels were determined with pseudoviruses of three Omicron subvariants (BA.1, BA.2, BA.4/5) (Fig. 2B). Fig. 2B shows that levels of nAbs elicited by ZSVG-02-O reduced by 2.6-, 3.8- and 6.0-fold for BA.2 and 16.5-, 24.3- and 6.2-fold for BA.4/5, respectively at 3 μg, 10 μg, and 30 μg doses.

T cell immune response in animals received two doses of ZSVG-02-O (3 μg, 10 μg, and 30 μg) with a 14-day interval was determined. Splenocytes were collected and analyzed 4 weeks after the second vaccination. Spike protein-specific cellular immunity was evaluated by intracellular staining of the cytokines induced by incubating the splenocytes with the full-length S protein of different variants. Fig. 3A–H show that ZSVG-02-O-elicited antigen-specific response in both $CD4^+$ and $CD8^+$ T cells, indicated by the elevated percentages of IFN-γ/$CD69^+$ T cells following the treatment with ancestral, Delta, or Omicron BA.1

Spike proteins, respectively. Parallel ELISpot assay for interleukin (IL)-2 expression in splenocytes further confirmed a strong immune response against the Omicron (BA.1) variant by ZSVG-02-O-immunized mice stimulated with Omicron Spike protein (Fig. 3I). Meanwhile, IL-5 was not significantly elevated across all samples (Fig. 3J), suggesting that ZSVG-02-O mainly induced a Spike-specific Th1 immune response rather than Th2. We found no T cell immunity against the nucleocapsid protein of the ancestral virus (Fig. 3D and H) in ZSVG-02-O-vaccinated animals. Similarly, the Delta-specific vaccine ZSVG-02 also induced significantly elevated cellular immune responses against Spike proteins of the ancestral, Delta, and Omicron variants but not the ancestral nucleocapsid protein. (Fig. S4).

Together, these results show that ZSVG-02 and ZSVG-02-O induce strong protective immune responses against SARS-CoV-2 variants at both humoral and cellular levels.

### 2.3. Heterologous boost of ZSVG-02-O following two-dose BBIBP-CorV primer induce strong protective immune response

Since a large proportion of the world had received inactivated whole-virus vaccines of ancestral strain, we further investigated whether boosting with the Omicron-specific ZSVG-02-O mRNA vaccines following an inactivated whole-virus vaccine could induce greater protective immune response against various VOCs. For that, BALB/c mice were first Intramuscularly (IM) immunized with two doses of BBIBP-CorV followed by one dose of ZSVG-02-O as a heterologous boost (Fig. 4A). Fig. 4B–C show the nAb levels determined with live viruses of the three strains following the two prime-boost regimes tested. Homologous BBIBP-CorV boost can produce adequate nAb levels against the ancestral strain and Delta variant but not for Omicron BA.1. A single ZSVG-02-O boost, however, can induce nAbs of comparable levels across all three strains. Fourteen days post ZSVG-02-O boost further increased the nAb levels compared to 7 days post immunization, especially against Omicron BA.1. Notably, the nAb levels induced by the single ZSVG-02-O boost following two-dose BBIBP-CorV prime show no obvious dose dependency, and the antibodies induced show the highest level against the ancestral strain. We also observed similar results against the Delta strain for the BBIBP-CorV/ZSVG-02 heteroboost (Fig. S5).

### 2.4. ZSVG-02-O heterologous boost protects mice from challenges by Delta and Omicron BA.1 viruses

Next, we tested the protection by the above ZSVG-02-O heterologous boost on ACE2-expressing transgenic mice, challenged with Delta or Omicron variant live viruses. The immunization scheme and experiment timing are shown in Fig. 5A. Fourteen days following the boost, the sera nAb levels were detected with live viruses of the Delta and Omicron strains (Fig. 5B). Then the animals were challenged intranasally with the viruses at a dose of 200 $CCID_{50}$. In the saline control group, we observed a significant body weight loss starting from Day 4 (Fig. 5C) after Delta or Omicron variant challenges. Four out of four mice died 6 days post
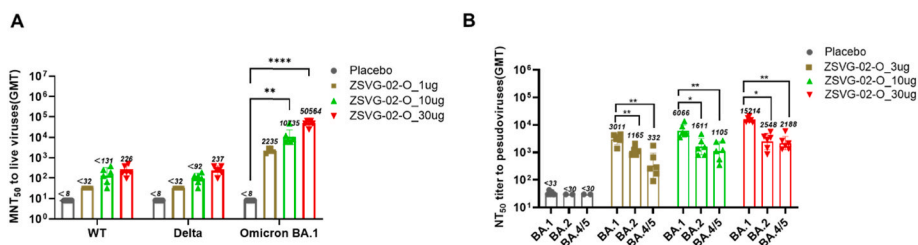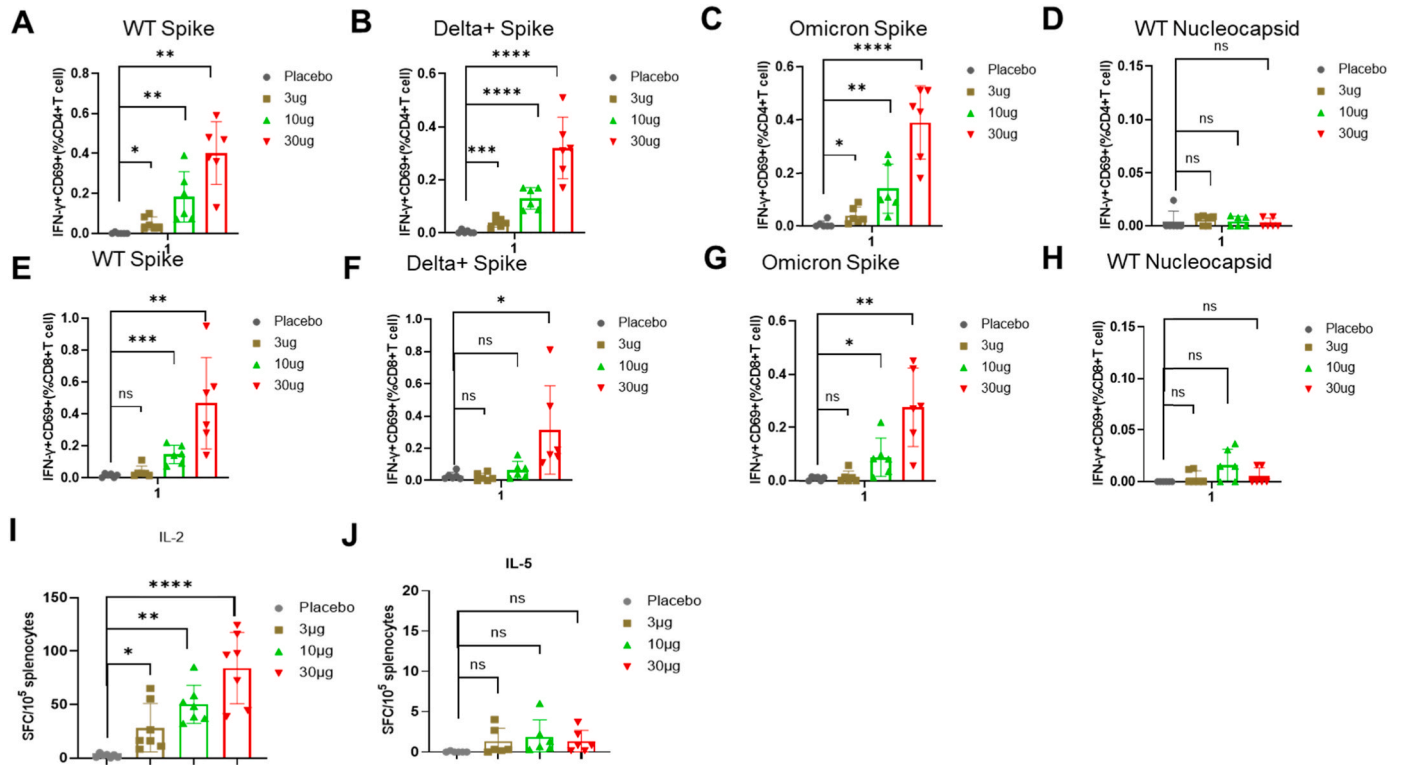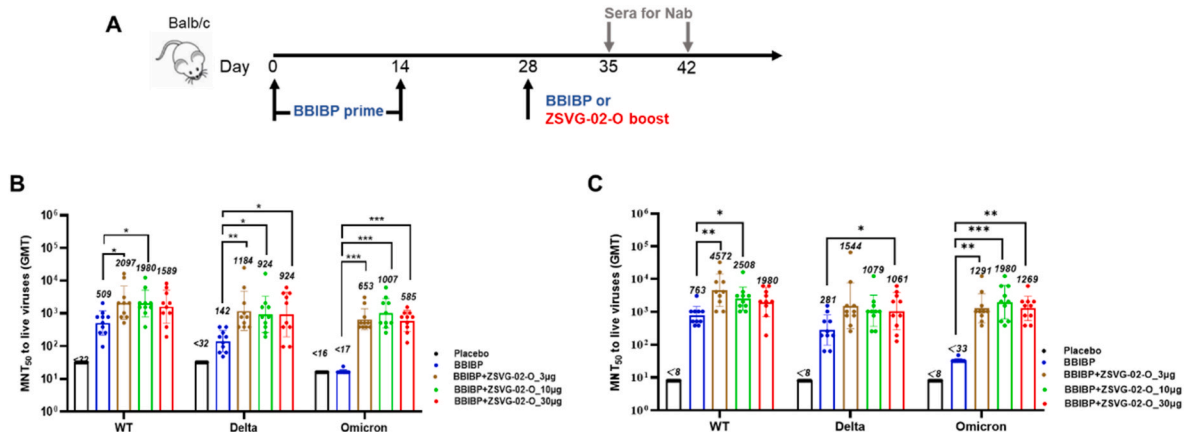


**Fig. 2.** Serological evaluation of ZSVG-02-O immunization in mice received 2 doses of ZSVG-02-O with a 14- or 21-day interval. (A) BALB/c mice (n = 6/group) were immunized with two doses of 1 μg, 10 μg and 30 μg ZSVG-02-O, 3 weeks apart, by intramuscular injection. GMT of neutralizing antibodies against live WT, Delta and Omicron BA.1 viruses one week after the second immunization. (B) BALB/c mice (n = 6/group) were immunized with two doses of 3 μg, 10 μg and 30 μg ZSVG-02-O, two weeks apart, by intramuscular injection. GMT of neutralizing antibodies against Omicron BA.1, BA.2 and BA.4/5 pseudoviruses two weeks after the second immunization. Data shown are geometric mean titers. Error bars represent geometric standard deviation. Data were analyzed by two-tailed nonparametric Kruskal-Wallis with a multiple comparison test. $P < 0.05$ was considered statistically significant. WT, ancestral strain, *$P < 0.05$, **$P < 0.01$, ****$P < 0.0001$. Saline is used as placebo.

**Fig. 3.** SARS-CoV-2 Spike-specific T-cell immune response in ZSVG-02-O-vaccinated mice received 2 doses of ZSVG-02-O with a 14-day interval.
BALB/c mice (n = 6/group) were immunized with two doses of 3 μg, 10 μg and 30 μg ZSVG-02-O, 2 weeks apart, by intramuscular injection. Splenocytes were collected 4 weeks post second immunization and stimulated with the indicated proteins of different variants for 48 h at concentration of 1 μg/mL (A)-(H) The proportions of IFN-γ/CD69$^+$ CD4$^+$ and CD8$^+$ T cells from ZSVG-02-O immunized mice stimulated with spike proteins or WT nucleocapsid protein. (I)-(J) ELISpot assay for IL-2 (I) and IL-5 (J) in splenocytes stimulated with Omicron Spike protein. Data are shown as mean ± SD, and analyzed by one-way ANOVA test (*$P < 0.05$, **$P < 0.01$, ***$P < 0.001$, ****$P < 0.0001$). WT, ancestral strain. SFC, spot forming cells. Saline is used as placebo.



**Fig. 4.** Serological evaluation of single-dose ZSVG-02-O boost following two-dose immunization of inactivated vaccine in mice
(A) Schematic diagram of immunization regimens. BALB/c mice (n = 10/group) were injected with two doses inactivated vaccine and a single dose of 3 μg,10 μg and 30 μg ZSVG-02-O with two-week interval. Neutralizing antibody titers were measured on seven days post vaccination (Day 35). (B) and fourteen days post vaccination (Day 42). (C). Data shown are geometric mean titers. Error bars represent geometric standard deviation. Data were analyzed by two-tailed nonparametric Kruskal-Wallis with a multiple comparison test. P < 0.05 was considered statistically significant. WT, ancestral strain.*$P < 0.05$, **$P < 0.01$, ***$P < 0.001$. Saline is used as placebo.

challenge in the Delta group. Two out of four mice died and the remaining two were severely sick 8 days post infection with the Omicron variant (Fig. 5D). No animal died or lost body weight in the ZSVG-02-O heterologous boost group 8 days post infection with Omicron. The 1 μg and 10 μg groups boosted with ZSVG-02-O showed moderate body weight loss in Delta variant-challenged animals, while the 30 μg group remained healthy. Furthermore, virus loads of both VOCs in

heterologously vaccinated animals fell significantly below the controls, measured by qRT-PCR tests on turbinate and lung tissue (Fig. 5E and F). By contrast, the BBIBP-CorV homologous boost group showed notable body weight loss after Delta variant challenge with no death observed. This group also survived Omicron challenge with no measurable body weight loss and showed reduced virus loads in tissues compared to the saline group (Fig. 5C–F). Overall, for the BBIBP-CorV primed mouse,
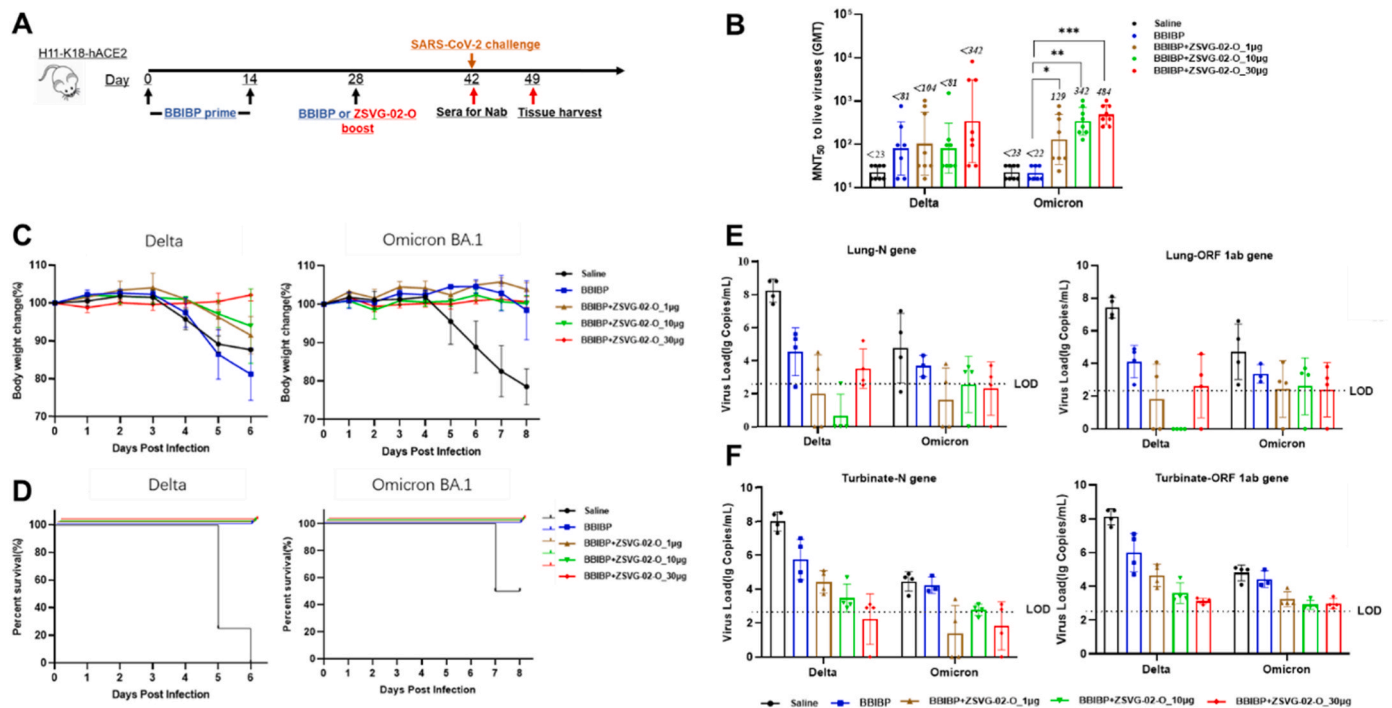
**Fig. 5. Protection against challenges of SARS-CoV-2 variants in BBIBP-ZSVG-02-O heterologous prime-boosted mice.** (A) Schematic diagram of immunization regimens. The ACE2-expressing transgenic mice (n = 8/group) were injected with two doses inactivated vaccine and a single dose of 1 μg, 10 μg and 30 μg ZSVG-02-O with two-week interval. Then the mice in each dose group were divided into two groups (n = 4/group) and challenged intranasally with live Delta and Omicron BA.1 viruses at a dose of 200 CCID$_{50}$. (B) GMT of neutralizing antibodies against Delta and Omicron BA.1 live viruses on the day of virus challenges (D42). Data shown are geometric mean titers. Error bars represent geometric standard deviation. Data were analyzed by two-tailed nonparametric Kruskal-Wallis with a multiple comparison test. (C) Body weight changes following virus challenges and (D) the survival rates post viral challenge. (E) - (F) qPCR detection of viral loads in lung tissue and turbinate. Data shown are mean plus SD. Data were analyzed by one-way ANOVA with a multiple comparison test. LOD: limit of Detection. $P < 0.05$ was considered statistically significant. *$P < 0.05$, **$P < 0.01$, ***$P < 0.001$. Saline is used as placebo.

ZSVG-02-O heterologous boost offered 100% protection against Omicron virus, superior to a third homologous BBIBP-CorV boost. The Delta-specific ZSVG-02 also produced similar results, albeit more biased towards protection against Delta, as shown in Fig. S6.

### 2.5. Two-dose ZSVG-02-O heterologous boosts induce more omicron-specific neutralizing antibodies

We further investigated immune responses of a two-dose heterologous boosts on BBIBP-CorV-primed mice. The immunization scheme and experiment timing are shown in Fig. 6A. The sera were collected 13 and 14 days following the 1st and 2nd boost, respectively. Fig. 6B and C compare nAb levels after 1st and 2nd boost for the BA.1 and BA.4/5 omicron subvariants. For the BA.1 variant, the second boost of BBIBP-CorV or 1 μg, 10 μg, 30 μg ZSVG-02-O induced 5.3-, 13.6-, 16.8-, and 10.6-fold nAb increases, respectively. For the BA.4/5 variant, the increases were 2.9-, 3.2-, 5.4-, and 3.1-fold. Thus, a second boost can noticeably increase nAbs against Omicron subvariants, especially the BA.1 subvariant. Further, compared to homologous boost (four shots of BBIBP-CorV), heterologous boost with ZSVG-02-O (two BBIBP-CorV + one or two ZSVG-02-O) induced much higher nAb levels for Omicron variants (Fig. 6B–C). For BA.1, a single ZSVG-02-O boost induced nAb levels 2.3- to 7.1-fold and a double boost further increased the difference to 5.9- to 12.7-fold depending on the mRNA dose. For BA.4/5, the gap reached 1.3- to 9.6-fold after a single boost and 1.4- to 10.3-fold after a second boost.

Since one ZSVG-02-O boost to BBIBP-CorV-primed mice produces similar levels of nAbs for all three VOCs (Fig. 4B and C), we wondered what population of antibodies, Omicron-specific or cross-reactive, this heterologous boost scheme produces. To investigate, we collected sera at Day 27 (pre-boost), Day 41 (13 days post 1st-boost) and Day 56 (14 days

post 2nd-boost), and depleted their antibodies that react to the ancestral RBD. The resulting IgG was titrated with Omicron BA.1 RBD to determine the percentages of IgG for non-ancestral RBD. Our results show that after a single ZSVG-02-O boost, depletion of the ancestral RBD-binding IgG resulted in 95–99% loss of total IgGs in sera collected (Fig. 6D). However, 2 weeks after the second boost with ZSVG-02-O, percentages of non-ancestral RBD-binding IgG increased to ~14%, 3- to 10- fold that of a single ZSVG-02-O boost. As a control, we found no change in the percentages of non-ancestral RBD-binding IgG for animals receiving two doses of homologous BBIBP-CorV boosts. These results indicate that a single ZSVG-02-O boost following the BBIBP-CorV prime mainly elevates levels of antibodies cross-reactive to both Omicron and the ancestral RBD, while the second ZSVG-02-O boost specifically increases the population of antibodies that recognize Omicron RBD but ignore the ancestral RBD.

### 3. Discussion

The highly transmissible Omicron variants represent the ongoing challenge of battling the pandemic globally. Our data reveal that the ZSVG-02-O codes a highly dynamic Omicron Spike antigen that frequents multiple conformations, unlike the ZSVG-02 coded Delta Spike antigen. Our result, alongside most other recent studies, explains why mutations in Omicron RBD facilitate its binding to ACE2, and hence spreads more rapidly than Delta (Shah and Woo, 2021; Golcuk et al., 2021). Our EM data also confirm that Omicron has evolved its Spike protein to adopt less stable thermodynamic states, presumably to facilitate evading host immune response while enhancing ACE2 interaction (Toelzer et al., 2020).

To counter these prevailing VOCs, this study introduces and evaluates the Delta-specific (ZSVG-02) and the Omicron-specific (ZSVG-02-O)
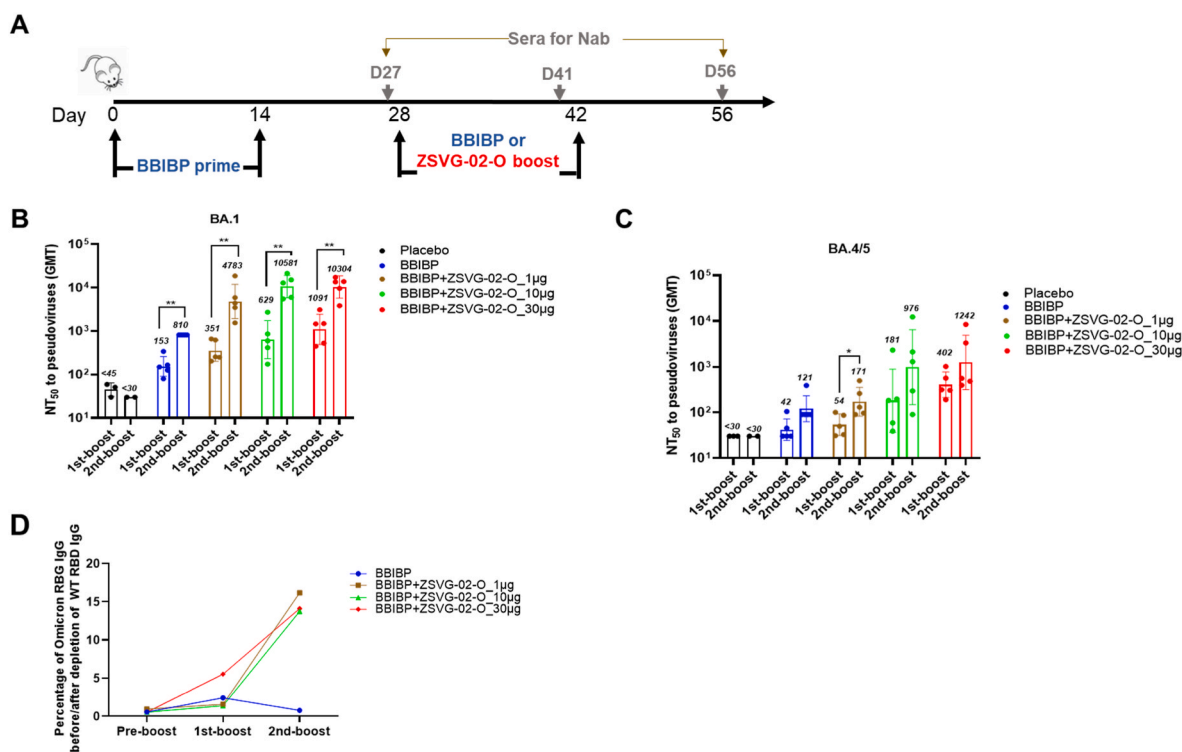
**Fig. 6. ZSVG-02-O boost induced Omicron-specific antibodies.** (A) Schematic diagram of immunization regimens. BALB/c mice (n = 5/group) were injected with two doses inactivated vaccine and two doses of 1 µg, 10 µg and 30 µg ZSVG-02-O with two-week interval. Sera samples were collected at D27 (pre-boost), D41 (1st-boost) and D56 (2nd-boost). (B) GMT of neutralizing antibodies against Omicron BA.1 pseudoviruses. (C) GMT of neutralizing antibodies against Omicron BA.4/5 pseudoviruses. (D) Percentage of Omicron RBD specific IgG after depletion of ancestral RBD-binding IgG. Data shown are geometric mean titers. Error bars represent geometric standard deviation. Data were analyzed by two-tailed nonparametric Mann-Whitney *U* test with a multiple comparison test. *P* < 0.05 was considered statistically significant. \**P* < 0.05, \*\**P* < 0.01. Saline is used as placebo.

mRNA vaccines. We demonstrate that they produce active antigen and induce a strong immune response in BALB/c mice with high neutralizing antibodies measured by live viruses. ZSVG-02 appears to induce higher neutralizing antibody levels for ancestral strain than ZSVG-02-O, probably due to the higher Spike protein homology between the Delta variant and the ancestral strain (Kumar et al., 2022; Simon-Loriere and Schwartz, 2022). ZSVG-02-O likely produces more Omicron-specific antibodies that target Spike conformations otherwise unfavorable in Delta and ancestral virus. However, the Omicron BA.1-based ZSVG-02-O can produce antibodies that cross-react to Omicron BA.2 and BA.4/5 (Fig. 2C), albeit with reduced activity due to progressive mutations in the two subvariants (Chen and Wei, 2022; Yu et al., 2022). Nevertheless, our results show that ZSVG-02-O can induce sufficient levels of neutralizing cross reactivity against all Omicron subvariants, providing both humoral and T cell immunity.

ZSVG-02-O-stimulated humoral immunity differs from its T cell immunity. Our data show that ZSVG-02-O induces humoral response that skewed to their home variant in naïve animals (Fig. 2). Conversely, T cell responses to the Spike proteins induced by ZSVG-02-O or ZSVG-02 appear similar across all three strains tested (Fig. 3 and S3). The discrepancy of cross-reactivity between humoral and cellular immunity also emerges from people who received Ad26.CoV2.S or BNT162b2, or from recently convalescent but unvaccinated COVID-19 patients. Sera from those showed "diminished neutralization capacity" for Omicron variant but had similar T cell immunity across the ancestral, Beta, Delta and Omicron (Keeton et al., 2022). T cell immunity provides protection through direct clearance of virus-infected cells by cytotoxic CD8^{+} T cells, or through enhancing humoral immunity by CD4^{+} T helper cells (Moss, 2022), without the need for humoral neutralizing antibodies. Clinically, higher levels of effector-associated transcripts in CD8^{+} T cell correlates with recovery from severe infections (Su et al., 2020). The

broad T cell immunity by vaccines may explain why ZSVG-02-O vaccination can protect animals from Delta virus challenges despite relatively lower nAb levels against the ancestral and Delta strains (Fig. 2A).

We have investigated a heterologous prime-boost strategy with ZSVG-02-O following BBIBP-CorV, which is one of the major inactivated virus vaccines used in China and many other countries. From our data, we conclude that the humoral immunity induced by the heterologous BBIBP-CorV/ZSVG-02-O prime-boost regime differs greatly from that induced by two-dose ZSVG-02-O in naïve animals. When the naïve animals were vaccinated with ZSVG-02-O only, the resulting nAb levels clearly biases towards the Omicron variant (Fig. 2). Conversely, a single ZSVG-02-O but not BBIBP-CorV boost following the two-dose BBIBP-CorV prime induces nAb levels comparable across all three strains (Fig. 4). Our results on heterologous boost with ZSVG-02-O agree with recent studies (Gagne et al., 2022; Kalnin et al., 2022) on Omicron specific boosts. Those studies show a single Omicron-specific boost also induce similar antibody titers across the multiple strains. Compared with Omicron-specific mRNA vaccines from Moderna (mRNA-1273.529) (Scheaffer et al., 2023) and BioNtech (Omi BA.1) (Muik et al., 2022), ZSVG-02-O produced almost identical Nab responses in naïve animals against WT, Delta and BA.1 VOCs. However, a heterologous BBIBP-CorV/ZSVG-02-O prime-boost strategy produced a broadened immune response more similar to the bivalent mRNA-1273.214 from Moderna (Scheaffer et al., 2023) and BioNtech (BNT162b2 +. Omi BA.1). Both bivalent mRNA and BBIBP-CorV/ZSVG-02-O prime-boost show improved response against VOCs absent in the vaccines (Scheaffer et al., 2023; Muik et al., 2022). To understand the reason underlying the broadened cross-activity by the ZSVG-02-O boost, we analyzed the composition of total IgG in the sera from animals received the single dose ZSVG-02-O following the BBIBP-CorV prime. We found that the vast majority of antibodies

induced by the first ZSVG-02-O boost were dual responders to both Omicron and ancestral RBDs. This result coincide with Gagne and co-workers' report that, in their mRNA1273 primed monkeys, a single mRNA Omicron-specific boost only activated B cells that were dual responsive to both ancestral strain and Omicron while few Omicron-specific B cells were detected (Gagne et al., 2022). Therefore, we postulated that a single ZSVG-02-O boost simply recalls the immunity built by the vaccine against the ancestral strain and "re-shapes" the IgG distribution to cross-react with Omicron, producing comparable nAb levels across all three strains tested. Thus, compared to two-dose immunization with Omicron-targeting vaccine alone, heterologous boost following vaccines for the ancestral strain can expand the breadth of immunity against more variants.

The immunity-broadening effect from BBIBP-CorV prime + ZSVG-02-O boost also manifested in enhanced T cell cross-reaction. In animals that received BBIBP-CorV vaccine followed by a single boost with the Delta-targeting ZSVG-02, the T cells show a strong response to the Nucleocapsid protein (N-protein) (Fig. S5H) that is absent in naïve animals vaccinated with either ZSVG-02-O or ZSVG-02 alone (Fig. 3 and S3). Thus, a Spike-specific ZSVG-02 boost seems to enhance existing anti-N-protein cellular immunity generated by the BBIBP-CorV prime, probably by a non-specific mechanism that causes general boosting of immune responses.

We further demonstrated that a second boost with ZSVG-02-O can significantly increase a population of Omicron-specific IgGs that do not cross-react with ancestral RBD (Fig. 6D). This suggests that new B cell populations that produce Omicron-specific antibodies may necessitate a second Omicron-targeting boost. Alternatively, the Omicron-specific B cell population was already induced by the first boost, only needing additional time to produce sufficient levels of Omicron-specific antibodies. Resolving this mechanism warrants further nAb depletion assays using different and/or prolonged time points. In addition, further analysis of both germline and peripheral B-cell populations and their receptors responsive to S protein of SARS-CoV-2 variants is necessary to reveal the mechanisms. Meanwhile, we look forward to clinical studies that compare a ZSVG-02-O single- or double-boost in their abilities to protect against all current VOCs, particularly the Omicron variants. In addition, 2 doses of ZSVG-02-O vaccination in naïve animals seemed to produce neutralizing antibody levels comparable or even higher than the 2xBBIBP+2xZSVG-02-O immunization regime. Because of no observed statistical significance between the two regimes, the difference may be within the experimental error. However, we cannot rule out the possibility of immune imprinting effect (Gao et al., 2023; Wheatley et al., 2021) caused by previous vaccinations of BBIBP vaccine, which needs further more detailed study. Meanwhile, the main advantage of heterologous prime-boost with the inactivated virus vaccine lies in the broadened breadth of the immune response against multiple variants.

Although homologous BBIBP-CorV prime-boost can partially protect the animals from Delta or Omicron BA.1 live viruses, we demonstrate that our heterologous immunization schemes offer complete protection against challenges by Delta and Omicron variants in a lethal ACE2-expressing mouse model. The BBIBP-CorV prime + ZSVG-02-O boost strategy produces higher nAb levels, broader T cell response, and hence more protection. It remains to be investigated whether a natural infection with Omicron variants in people previously vaccinated with the inactivated ancestral vaccines will produce similar immune responses as that by Omicron-targeting vaccine. In conclusion, our study proves that ZSVG-02-O effectively protects against Omicron infection as a stand-alone vaccine. More importantly, populations previously vaccinated with inactivated whole-virus of the ancestral strain, such as the BBIBP-CorV, can receive full benefits from a heterologous boost regime with ZSVG-02-O. The boost consolidates their previous primes and provides new resistance to Omicron variants by broadening both humoral and cellular immunity to cover all prevailing VOCs.

## 4. Materials and methods

### 4.1. Cryo-electron microscopy analysis

Both Spike proteins were expressed in HEK293F cells as previously reported (Gobeil et al., 2022; Hong et al., 2022). The eluted proteins were concentrated using an Amicon Ultra centrifugal device (Millipore) with 100 kDa MW cut-off, and then applied to a Superose 6 5/150 column (Cytiva) for further purification. The peak fractions corresponded to S glycoprotein trimers were used for cryo-EM sample preparations. The proteins were concentrated to 0.75 mg/mL: An aliquot of 4 μL protein sample of Spike protein was applied onto a glow-discharged 300 mesh grid (Quantifoil Au R1.2/1.3) and GraFuture™-RGO grid which was supported with a thin layer of RGO (reduced graphene oxide), blotted with filter paper for 3.0 s using 3 blot force, and then plunge-frozen in liquid ethane using a Thermo Fisher Vitrobot Mark IV. Cryo-EM micrographs were collected on a 300 kV Thermo Fisher Titan Krios G4 electron microscope equipped with a Falcon4 direct detection camera. The micrographs were collected at a calibrated magnification of 96,000X, yielding a pixel size of 0.86 Å at a counting mode. In total, 5, 248 micrographs were collected at an accumulated electron dose of 57.3 e-Å-2 s-1 on each micrograph that was fractionated into a stack of 32 frames with a defocus range of −1.0 to −2.0 μm. Beam-induced motion correction was performed on the stack of frames using MotionCorr2 (Zheng et al., 2017). The contrast transfer function (CTF) parameters were determined by CTFFIND4 (Rohou and Grigorieff, 2015). A total of 5,248 good micrographs were selected for further data processing using the cryoSPARC software program according to standard procedures (Punjani et al., 2017). Finally, the first conformation (2 up RBDs 1 down RBDs) was constructed from 432,771 particles and reconstructed at a global resolution of 2.82 Å based on the gold-standard Fourier shell correlation criterion at FSC = 0.143 after refinement and CTF refinement. Another conformation (1 up RBDs 2 down RBDs) was executed by the same method, and the final resolution was 3.05 Å constructed from 346,652 particles. The molecular models were built by fitting a predicted structure of Omicron Spike protein from AlphaFold2 into the density map using UCSF Chimera (Pettersen et al., 2004; Bryant et al., 2022), followed by a manual model building of Omicron Spike protein in COOT (Bond et al., 2020) and real space refinement in PHENIX (Adams et al., 2010). The model statistics were listed in Supplementary Table 1.

### 4.2. mRNA synthesis

mRNA was synthesized following standard procedures (Baronti et al., 2018; Beckert and Masquida, 2011; Whitley et al., 2021). Namely, we used T7 RNA polymerase in the presence of a CleanCap Reagent AG (3' OMe) (TriLink) on linearized plasmids encoding codon-optimized SARS-CoV-2 gene. After transcription, the mRNA was purified by magnetic particles, flash frozen, and stored at −80 °C until further use.

### 4.3. mRNA encapsulation

ZSVG-02 or ZSVG-02-O mRNA with four-component lipid mixture were fabricated as mRNA-LNPs using a microfluidic nanoprecipitation process in which an aqueous solution of mRNA was rapidly mixed with a solution of lipids. Next, the encapsulated mRNA was diluted to 0.5 mg/mL. Finally, the product was sterile filtered through a 0.22 μm Sartopore polyethersulfone (PES) membrane and aliquots were subsequently stored at room temperature or frozen at −80 °C (1.0 mL fill).

### 4.4. mRNA-LNP characterization

Frozen vials were taken from storage and equilibrated to room temperature before characterizations. Particle size, polydispersity (PDI), and Zeta-potential of mRNA-LNPs were measured by dynamic light scattering (Malvern Nano ZS Zetasizer). Diameters are reported as Z-

average. Encapsulation efficiency (E.E.) of mRNA in the LNP is defined as the mass ratio of encapsulated mRNA/total mRNA in the final mRNA-LNP product. Nucleic acids such as mRNA can be detected quantitatively using specific intercalating fluorescent dyes. The concentration of mRNA was calculated from a calibration curve generated using the mRNA standards. The relative proportion of encapsulated mRNA in mRNA-LNPs was determined via the ratio of the fluorescence signal in the absence vs. the presence of a surfactant that dispersed the LNPs. The signal in the absence of surfactant indicated the level of free mRNA while the signal in the presence of the surfactant provided a measure of the total mRNA in the sample.

To evaluate the quality and stability of the encapsulated mRNA, we compared ambient-stored LNPs with that after freeze/thaw cycles from −80 °C. After freeze-thaw from −80 °C, we observed almost identical size (~90 nm) and monodispersity (PDI = 0.034) (Fig. S1A) as the samples stored at room temperature (Fig. S1B). We also measured similar encapsulation efficiency (E.E.) of 99.63% (ambient) and 98.02% (-80 °C), showing both high purity and stability of our LNPs (Fig. S1B). The slight negative Zeta potential of the mRNA-LNPs (-3 to −4 mV) can facilitate intracellular uptake (Fig. S1C), as recommended by other common verified mRNA vaccine formulations (Huang et al., 2021; Karpenko et al., 2021). Our LNP characterization results show that our procedure and formulation can produce monodispersed and stable mRNA-LNPs.

### 4.5. Cell culture

HEK293T/17 cells were cultured in Dulbecco's Modified Eagle's Medium (DMEM, Gibco, USA) supplemented with 10% fetal bovine serum (FBS). The cells were maintained in a 37 °C humidified incubator supplied with 5% $CO_2$. The Vero cells (ATCC, TL-CCL-81.4) were cultured in DMEM (Gibco, USA) supplemented with 10% newborn calf serum (NCS, Gibco, USA), 50 U/mL penicillin-streptomycin (Gibco, USA), in a 37 °C incubator with 5% $CO_2$.

### 4.6. Culture and transfection of human DCs

Frozen aliquots of human peripheral blood mononuclear cells (PBMCs) from healthy donors were purchased from Shanghai Saili Biotech. Six days before transfection, frozen PBMCs were thawed and resuspended in serum-free RMPI 1640 medium. Then PBMCs were plated in the cell culture dish with the density of $2 \times 10^6$ cells/mL and incubated for 2 h at 37 °C. Next, the PBMCs were gently washed with warmed phosphate-buffered saline (PBS) three times. The adherent cells were cultured with RPMI 1640 medium supplemented with 10% FBS, human recombinant granulocyte-macrophage colony-stimulating factor (GM-CSF, 50 ng/mL R&D Systems, 7954-GM-020/CF), and interleukin-4 (IL-4, 50 ng/mL, R&D Systems, 6507-IL-025/CF) for 5 days. Then, the PBMC-derived immature dendritic cells (DCs) were replated into a 96-well plate. Cells were transfected with naked mRNA (500 ng/well), or 5′ppp-dsRNA (2500 ng/well; InvivoGen, tlrl-3prna), or 3p-hpRNA (Invivogen, tlrl-hprna-100), or PolyI:C (2500 ng/well; InvivoGen, tlrl-picw), or LNP-mRNA (500 ng/well) for 24 h. The supernatant was collected for ELISA.

### 4.7. Flow cytometry analysis

The HEK293T/17 cells were transfected with ZSVG-02 or ZSVG-02-O mRNA, either naked or LNP-encapsulated, at 0.75 μg/well. After 24 h, the cells were harvested by 0.25% Trypsin-EDTA (Gibco) treatment and were blocked with 5% goat serum for 10 min 100 μL biotinylated recombinant human ACE2 protein (His AVI Tag, 0.25 μg/μL, 1:100) (Sinobiology) and recombinant streptavidin protein (phycoerythrin) (Abcam) were used as the primary and secondary antibodies for ACE-2 protein detection. For RBD staining, PE-labeled Anti-SARS-CoV-2 Spike RBD neutralizing antibody (Acro) was used.

When antigen specific T cells are engaged with pMHC from APC, T cells will be activated and express cytokines (Gauduin et al., 2006). Therefore, since CD69^{+} IFN-γ cells were more representative spike antigen specific T cells, they present a good indicator of protective cellular immunity. For T cell intracellular cytokine staining, splenocytes were isolated and resuspended with RPMI 1640 medium supplemented with 10% FBS. 2 μg/mL Spike trimer protein or peptide pool was added to media separately. Splenocytes were stimulated for 42 h at 37 °C before adding 2 mM monensin (Biolegend #420701) for an additional 6 h. Then, splenocytes were collected by centrifuge and subjected to staining process. Firstly, cells were stained with live/dead cell dye (Zombie NIR™, Biolegend) as well as antibodies to cell surface markers (anti-45 AF700 [Biolegend, 147716], anti-CD3e FITC [Biolegend, 100306], anti-CD4 BV786 [Biolegend, 100552], anti-CD8 BV605 [Biolegend, 100744], anti-CD69 APC [Biolegend, 104514]) at 4 °C for 30 min. Next, stained cells were washed with PBS, fixed and permeabilized using the Cytofix/Cytoperm™ kit according to manufacturer's protocol (BD Bioscience, 554715). Finally, cells were stained with antibodies of cytokines (anti-IFN-γ [Biolegend, 505808], anti-IL-2 [Biolegend, 503822], anti-IL-13 PE/Cy7 [Invitrogen, 25-7133-82]) at 4 °C for 1 h, and stored in PBS before analysis (Fig. S8).

For effector cell and DC staining, uncultured splenocytes were incubated with antibodies (anit-CD45 APC/Cy7 [Biolegend, 103116], anti-CD11C FITC [Biolegend 117306], anti-CD3e Percp5.5 [BD Pharmingen, 551163], anti-IA/IE AF700 [Biolegend 107622], anti-CD4B V786 [Biolegend, 100551], anti-CD8 BV605 [Biolegend, 100744], anti-CD44 PE [Biolegend, 103008], anti-CD62L BV650 [Biolegend, 104453], anti-CD69 APC [Biolegend, 104514]) at 4 °C for 30 min. The cells were then washed with PBS and subjected to flow cytometry analysis (Beckman, CytoFLEXLX). General gating strategies are shown in Fig. S7.

### 4.8. Enzyme-linked immunosorbent assay (ELISA)

To measure the secreted cytokine levels of IFN-α and TNF-α, the dendritic cell supernatant was collected at 24 h post transfection with ZSVG-02 or ZSVG-02-O. Human TNF-α Ultrasensitive ELISA Kit (Invitrogen , KHC3014 [96 tests] and Human IFNα ELISA Kit [Invitrogen , BMS216TEN]) were used for cytokine quantification.

### 4.9. Determination of viral titers by cell culture infectious dose 50% assay ($CCID_{50}$)

Virus-containing samples, Wild-type/Prototype/WIV04 (NCBI Reference Sequence: NC_045512.2), Delta (Genebank accession no. OU428631.1) and Omicron (GISAID accession no. EPI_ISL_7138045) were 10-fold serially diluted in infection medium DMEM +2.5% NCS +1% penicillin-streptomycin and then transferred into a 96-well plate with approximately 2 - 3 × 10^5 Vero cells in each well with 8 replicates per sample. After 4 days of culture in a 37 °C incubator with 5% $CO_2$, cytopathic effect (CPE) was observed for the quantification of the median tissue culture infectious dose. The virus titer was calculated by the Karber method (Ramakrishnan, 2016).

### 4.10. Cell lysate preparation and Western blotting

The 293T/17 cells were transfected with ZSVG-02 or ZSVG-02-O mRNA produced by in vitro transcription (IVT), mock (empty lipofectamine 3000) and pcDNA3.1(−) plasmid-expressing S protein, respectively. After 24 h, the cells were collected and lysed with RIPA buffer (Beyotime, P0013B). Equal amounts of protein samples were then separated by 10% sodium dodecyl sulfate-polyacrylamide gel electrophoresis (SDS-PAGE) followed by transfer to polyvinylidene fluoride (PVDF) membranes (Millipore, Billerica, MA, USA). The membranes were first blocked with 5% skim milk for 1 h and then incubated with the primary antibodies of SARS-CoV-2 ( 2019-nCoV ) Spike RBD Antibody

(Sinobiology, 40592-T62-100) for 2 h at 37 °C. After TBS-T (0.1% v/v) washing and incubation with the secondary antibodies of goat anti-rabbit IgG-Fc (HRP) (Sinobiology, SSA003), the protein bands were detected by LumiQ HRP Substrate solution (Share-bio, SSA003) and imaged with ChemiDoc™MP imaging system (Bio-Rad, USA)

### 4.11. Pseudovirus neutralization assay

The pseudovirus neutralization assays were performed according to protocols described previously (Su et al., 2020). Briefly, serially diluted mouse serum samples were mixed with SARS-CoV-2 pseudoviruses (Vazyme Biotech Cat.# DD1402, DD1458, DD1768) in a 96-well plate and incubated at 37 °C for 1 h. Next, HEK293-ACE2 cells (Vazyme Biotech Cat.# DD1401) were added to each pseudovirus-containing well and incubated at 37 °C for 48 h. After incubation, the supernatants were removed and luciferase assay was performed with Bio-Lite™ Luciferase assay reagents (Vazyme Biotech, Cat.#DD1201). The neutralization antibody (nAb) titer was calculated and presented as half maximal effective concentration (EC50). For each assay, the pseudoviruses kit-included standard samples were used as positive and negative controls.

### 4.12. ELISpot assay

For ELISpot, splenocytes were isolated and resuspended with CTL-Test™ Medium containing CTL Serum-free Media with 1% Penicillin-Streptomycin (Gibco, Cat# 15140122) and 1% fresh L-glutamine (Beyotime Biotechnology, Cat# C0212). IL-2- and IL-5-positive spleno-cytes was performed according to the manufacturer's instructions for the ELISpot assay (Cellular Technology Ltd, USA). Briefly, 96-well plates were precoated with both anti-mouse IL-2 and IL-5 monoclonal anti-bodies. $3 \times 10^5$ cells of isolated mouse splenocytes per well were stim-ulated at 37 °C for 48 h using 1 μg/mL Spike trimer protein (ACRO, Cat # SPN-C52Hz). Wash plates two times with PBS and then two times with 0.05% Tween-PBS, detection antibodies were added and incubated at room temperature for 2 h. After three times washing, Tertiary Solution were added and incubated at room temperature for 30 min. Finally, the plates were washed two times with 0.05% Tween-PBS and then two times with distilled water. Add Blue Developer Solution and incubate at room temperature for 15 min. The spots were counted under CTL ImmunoSpot® Analyzers (Cellular Technology Ltd, USA).

### 4.13. Neutralization assay with live virus

Serum samples were diluted 1 in 16 in DMEM supplemented with 2.5% NCS, 50 U/mL penicillin-streptomycin (Gibco, USA), and then were added into an equal volume ( 0.05 mL/well ) of challenge virus solution (100 CCID$_{50}$ virus). After neutralization in a 37 °C incubator for 2 h, cell suspension with the virus was added into the 96-well plates (0.1 mL/well), which were cultured in a CO$_2$ incubator at 37 °C for 3–5 days. The assay of each serum was performed in 2 replicates, and the Karber method (Ramakrishnan, 2016) was used to calculate the neutralization endpoint. For each assay, a ZSVG-02-O immunized rabbit serum with known titer of neutralizing antibodies was used as the internal control.

### 4.14. Mouse vaccination

All experiments were approved by Jiangsu Provincial Department of Science and Technology with an approval number of SYXK (Su) 2020-0041. BALB/c mice of 8 weeks of age purchased from China Jiangsu Huachuang Sino were immunized intramuscularly (IM) with ZSVG-02 or ZSVG-02-O on days indicated. Blood samples were collected for neutralizing antibody (nAb) detection and mice were harvested for T cell immunity experiments. For pre-immunization with BBIBP-CorV (0.5 mL, 6.5 U each tube), 100 μL BBIBP-CorV/mouse was IM-administered at Day 1 and Day 14, followed by ZSVG-02 or ZSVG-02-O boosting at Day

28. Mice were harvested at Day 42 for T cell immunity experiments.

### 4.15. Mouse challenge with live SARS-CoV-2 Delta and Omicron BA.1 variants

The effect of *in vivo* protection by ZSVG-02 or ZSVG-02-O vaccination were assessed by using a *H11-K18-hACE2* mouse model with C57BL/6JGpt genetic background purchased from China GemPharmatec (Cat. #T037657) (Su et al., 2020; Bai et al., 2021; Zhang et al., 2020; McCray et al., 2007). Briefly, groups of 3- to 4-month-old male mice were anaesthetized with isoflurane, followed by intranasal inoculation with 200 CCID$_{50}$ of Delta or Omicron variant. Survival and body weight of the mice were monitored daily, and all animals were sacrificed upon death or at 6 or 8 dpi for harvesting lung tissues for virological assessment, pathological and histological examinations. Turbinate and lung tissues were subjected to qPCR viral load detection. The limit of detection (LOD) was approximately 2.7 Log copies/mL.

### 4.16. Removal of ancestral strain RBD-binding IgG

The RBD-binding antibodies against the ancestral strain variant were depleted by using magnetic beads coated with the RBD fragment of ancestral strain SARS-CoV-2 (AcroBiosystems, MBS-K002). According to the manufacturer's protocol, the beads were resuspended in ultrapure water at 1 mg beads/mL then washed 2 times in PBS with 0.05% BSA. The vaccine-immunized sera were diluted 8 times with 10 μL serum +70 μL 0.05% BSA/PBS based on the manufacturer-reported binding ca-pacity of 40 μg anti-RBD antibodies per mg beads. 80 μL beads were added to a tube and placed on the magnetic separator (Vazyme, CM101) for 1–2 min to remove the supernatant. Then, 80 μL of diluted serum was added to the tube and rotated at 4 °C for 24 h. The antibodies that bound RBD from the supernatant were separated by the magnetic separator, the supernatant was collected for another 80 μL beads for the second round of depletion to ensure full depletion of ancestral strain RBD-binding antibodies. The supernatants following the second depletion were collected and titrated for IgG that bind to Omicron RBD as described below.

### 4.17. Serum antibody measurement by ELISA

The IgG ELISAs for RBD were conducted by using Antibody IgG Titer Serologic Assay Kit (AcroBiosystems, RAS-T059). According to the manufacturer's protocol, the microplate of the kit was pre-coated with SARS-CoV-2 Spike RBD protein. Two-fold serial dilutions of sera were performed (serum dilution of D27 beginning at 1 in 25, serum dilution of D41 and D56 beginning at 1 in 250) in dilution buffer. Saline group serum was used as negative control and diluted at 1 in 100. 100 μL of diluted samples were added to the microplate and incubated at 37 °C for 1 h. After 3 washes, 100 μL HRP-goat anti-mouse IgG secondary anti-bodies were added and incubate at 37 °C for 1 h. After an additional 5 washes, 100 μL substrate solution were added to each well and incubate at 37 °C for 20 min in the dark. Next, 50 μL of stop solution was added to each well. OD450 and OD630 were read on a Tecan Spark plate reader. The cut-off value was 0.1. The value of OD450-OD630 is greater than or equal to cut-off value is the positive reading, otherwise it is the negative reading. The antibody titer of the sample corresponds to the highest dilution factor that still yields a positive reading.

### 4.18. Statistical analysis

Data were tested for statistical normality and the results were used to apply the appropriate statistical test. The Kruskal-Wallis tests and Mann-Whitney U tests were used for non-parametric data and one-way ANOVA tests and Student's *t*-tests for parametric data. All the statistical analyses were performed using SPSS Version 21.

## Author contributions

WJ and XMY. designed and funded the research; WJ analyzed data; CL, YTZ, ZJW, ZBY, FJH, FL, GHY, RJC, LXL, JX, XW, KL, JD, XGL, QZ, CXH, P.P, RZ, XHC performed research; CL, YTZ, ZBY, FL, JX, GHY, RJC, ZJW and WJ prepared the manuscript; the rest of authors participated and performed the research.

## Declaration of competing interest

ZBY, FJH, JD, XHL, JX, XWH, HH, RZ, XHC and WJ are or was employees of Virogin. The rest of authors are employees of CNBG or its subsidiary companies.

## Data availability

No data was used for the research described in the article.

## Appendix A. Supplementary data

Supplementary data to this article can be found online at https://doi.org/10.1016/j.antiviral.2023.105556.

## References

Adams, P.D., et al., 2010. PHENIX: a comprehensive Python-based system for macromolecular structure solution. Acta Crystallogr D Biol Crystallogr 66 (Pt 2), 213–221.

Al Kaabi, N., et al., 2022. The incidence of COVID-19 infection following emergency use authorization of BBIBP-CORV inactivated vaccine in frontline workers in the United Arab Emirates. Sci. Rep. 12 (1), 490.

Andreano, E., et al., 2021. Extremely potent human monoclonal antibodies from COVID-19 convalescent patients. Cell 184 (7), 1821–1835.e16.

Baden, L.R., et al., 2021. Efficacy and safety of the mRNA-1273 SARS-CoV-2 vaccine. N. Engl. J. Med. 384 (5), 403–416.

Bai, L., et al., 2021. Coinfection with influenza A virus enhances SARS-CoV-2 infectivity. Cell Res. 31 (4), 395–403.

Baronti, L., et al., 2018. A guide to large-scale RNA sample preparation. Anal. Bioanal. Chem. 410 (14), 3239–3252.

Beckert, B., Masquida, B., 2011. Synthesis of RNA by in vitro transcription. Methods Mol. Biol. 703, 29–41.

Bond, P.S., Wilson, K.S., Cowtan, K.D., 2020. Predicting protein model correctness in Coot using machine learning. Acta Crystallogr D Struct Biol 76 (Pt 8), 713–723.

Bryant, P., Pozzati, G., Elofsson, A., 2022. Improved prediction of protein-protein interactions using AlphaFold2. Nat. Commun. 13 (1), 1265.

Chansaenroj, J., et al., 2022. Immunogenicity following two doses of the BBIBP-CorV vaccine and a third booster dose with a viral vector and mRNA COVID-19 vaccines against Delta and omicron variants in prime immunized adults with two doses of the BBIBP-CorV vaccine. Vaccines (Basel) 10 (7).

Chen, J., Wei, G.W., 2022. Omicron BA.2 (B.1.1.529.2): High Potential for Becoming the Next Dominant Variant. J. Phys. Chem. Lett. 13 (17), 3840–3849.

Desingu, P.A., Nagarajan, K., Dhama, K., 2022. Emergence of Omicron third lineage BA.3 and its importance. J. Med. Virol. 94 (5), 1808–1810.

Ella, R., et al., 2021. Safety and immunogenicity of an inactivated SARS-CoV-2 vaccine, BBV152: a double-blind, randomised, phase 1 trial. Lancet Infect. Dis. 21 (5), 637–646.

Flemming, A., 2022. Omicron, the great escape artist. Nat. Rev. Immunol. 22 (2), 75.

Gagne, M., et al., 2022. mRNA-1273 or mRNA-Omicron boost in vaccinated macaques elicits similar B cell expansion, neutralizing responses, and protection from Omicron. Cell 185 (9), 1556–1571.e18.

Gao, B., et al., 2023. Repeated Vaccination of Inactivated SARS-CoV-2 Vaccine Dampens Neutralizing Antibodies against Omicron Variants in Breakthrough Infection. Cell Research.

Gauduin, M.C., et al., 2006. Induction of a virus-specific effector-memory CD4+ T cell response by attenuated SIV infection. J. Exp. Med. 203 (12), 2661–2672.

Gobeil, S.M., et al., 2022. Structural diversity of the SARS-CoV-2 Omicron spike. Mol Cell 82 (11), 2050–2068.e6.

Golcuk, M., Yildiz, A., Gur, M., 2021. The Omicron Variant Increases the Interactions of SARS-CoV-2 Spike Glycoprotein with ACE2. bioRxiv, p. 2021.

Heath, P.T., et al., 2021. Safety and efficacy of NVX-CoV2373 Covid-19 vaccine. N. Engl. J. Med. 385 (13), 1172–1183.

Hong, Q., et al., 2022. Molecular basis of receptor binding and antibody neutralization of Omicron. Nature 604 (7906), 546–552.

Huang, Q., et al., 2021. A single-dose mRNA vaccine provides a long-term protection for hACE2 transgenic mice from SARS-CoV-2. Nat. Commun. 12 (1), 776.

Kalnin, K.V., et al., 2022. Pan-SARS neutralizing responses after third boost vaccination in non-human primate immunogenicity model. Vaccine 40 (9), 1289–1298.

Karpenko, L.I., et al., 2021. Delivery of mRNA vaccine against SARS-CoV-2 using a polyglucin:spermidine Conjugate. Vaccines (Basel) 9 (2).

Keeton, R., et al., 2022. T cell responses to SARS-CoV-2 spike cross-recognize Omicron. Nature 603 (7901), 488–492.

Kuhlmann, C., et al., 2022. Breakthrough infections with SARS-CoV-2 omicron despite mRNA vaccine booster dose. Lancet 399 (10325), 625–626.

Kumar, S., et al., 2022. Omicron and Delta variant of SARS-CoV-2: a comparative computational study of spike protein. J. Med. Virol. 94 (4), 1641–1649.

Liu, L., et al., 2021. Striking antibody evasion manifested by the Omicron variant of SARS-CoV-2. Nature.

Mallapaty, S., 2021. China's COVID vaccines are going global - but questions remain. Nature 593 (7858), 178–179.

McCray Jr., P.B., et al., 2007. Lethal infection of K18-hACE2 mice infected with severe acute respiratory syndrome coronavirus. J. Virol. 81 (2), 813–821.

Moss, P., 2022. The T cell immune response against SARS-CoV-2. Nat. Immunol. 23 (2), 186–193.

Muik, A., et al., 2022. Exposure to BA.4/5 S protein drives neutralization of Omicron BA.1, BA.2, BA.2.12.1, and BA.4/5 in vaccine-experienced humans and mice. Sci Immunol 7 (78), eade9888.

Ophinni, Y., et al., 2020. COVID-19 vaccines: current status and implication for use in Indonesia. Acta Med. Indones. 52 (4), 388–412.

Pegu, A., et al., 2021. Durability of mRNA-1273 vaccine-induced antibodies against SARS-CoV-2 variants. Science 373 (6561), 1372–1377.

Pettersen, E.F., et al., 2004. UCSF Chimera–a visualization system for exploratory research and analysis. J. Comput. Chem. 25 (13), 1605–1612.

Polack, F.P., et al., 2020. Safety and efficacy of the BNT162b2 mRNA Covid-19 vaccine. N. Engl. J. Med. 383 (27), 2603–2615.

Punjani, A., et al., 2017. cryoSPARC: algorithms for rapid unsupervised cryo-EM structure determination. Nat. Methods 14 (3), 290–296.

Qu, P., et al., 2022. Neutralization of the SARS-CoV-2 Omicron BA.4/5 and BA.2.12.1 Subvariants. N Engl J Med.

Ramakrishnan, M.A., 2016. Determination of 50% endpoint titer using a simple formula. World J. Virol. 5 (2), 85–86.

Rohou, A., Grigorieff, N., 2015. CTFFIND4: fast and accurate defocus estimation from electron micrographs. J. Struct. Biol. 192 (2), 216–221.

Scheaffer, S.M., et al., 2023. Bivalent SARS-CoV-2 mRNA vaccines increase breadth of neutralization and protect against the BA.5 Omicron variant in mice. Nat. Med. 29 (1), 247–257.

Shah, M., Woo, H.G., 2021. Omicron: a heavily mutated SARS-CoV-2 variant exhibits stronger binding to ACE2 and potently escapes approved COVID-19 therapeutic antibodies. Front. Immunol. 12, 830527.

Simon-Loriere, E., Schwartz, O., 2022. Towards SARS-CoV-2 serotypes? Nat. Rev. Microbiol.

Stamatatos, L., et al., 2021. mRNA vaccination boosts cross-variant neutralizing antibodies elicited by SARS-CoV-2 infection. Science 372 (6549), 1413–1418.

Su, Y., et al., 2020. Multi-omics resolves a sharp disease-state shift between mild and moderate COVID-19. Cell 183 (6), 1479–1495.e20.

Tada, T., et al., 2021. Comparison of Neutralizing Antibody Titers Elicited by mRNA and Adenoviral Vector Vaccine against SARS-CoV-2 Variants. bioRxiv.

Tegally, H., et al., 2022. Emergence of SARS-CoV-2 omicron lineages BA.4 and BA.5 in South Africa. Nat. Med.

Thakur, V., Ratho, R.K., 2021. Omicron (B.1.1.529): a new SARS-CoV-2 variant of concern mounting worldwide fear. J. Med. Virol.

Toelzer, C., et al., 2020. Free fatty acid binding pocket in the locked structure of SARS-CoV-2 spike protein. Science 370 (6517), 725–730.

van der Straten, K., et al., 2022. Antigenic cartography using sera from sequence-confirmed SARS-CoV-2 variants of concern infections reveals antigenic divergence of Omicron. Immunity 55 (9), 1725–1731.e4.

Wang, H., et al., 2020. Development of an inactivated vaccine Candidate, BBIBP-CorV, with potent protection against SARS-CoV-2. Cell 182 (3), 713–721.

Wang, H., et al., 2022. mRNA based vaccines provide broad protection against different SARS-CoV-2 variants of concern. Emerg. Microb. Infect. 11 (1), 1550–1553.

Watanabe, Y., et al., 2021. Native-like SARS-CoV-2 spike glycoprotein expressed by ChAdOx1 nCoV-19/AZD1222 vaccine. ACS Cent. Sci. 7 (4), 594–602.

Weigang, S., et al., 2021. Within-host evolution of SARS-CoV-2 in an immunosuppressed COVID-19 patient as a source of immune escape variants. Nat. Commun. 12 (1), 6405.

Wheatley, A.K., et al., 2021. Immune imprinting and SARS-CoV-2 vaccine design. Trends Immunol. 42 (11), 956–959.

Whitley, J., et al., 2021. Development of mRNA manufacturing for vaccines and therapeutics: mRNA platform requirements and development of a scalable production process to support early phase clinical trials. Transl. Res. 242, 38–55.

Wu, K., et al., 2021. mRNA-1273 Vaccine Induces Neutralizing Antibodies against Spike Mutants from Global SARS-CoV-2 Variants. bioRxiv.

Yadav, T., et al., 2020. Recombinant vaccines for COVID-19. Hum. Vaccines Immunother. 16 (12), 2905–2912.

Yamasoba, D., et al., 2022. Virological characteristics of the SARS-CoV-2 Omicron BA.2 spike. Cell 185 (12), 2103–2115.

Yu, J., et al., 2022. Comparable Neutralization of the SARS-CoV-2 Omicron BA.1 and BA.2 Variants. medRxiv.

Zhang, S., et al., 2020. SARS-CoV-2 binds platelet ACE2 to enhance thrombosis in COVID-19. J. Hematol. Oncol. 13 (1), 120.

Zheng, S.Q., et al., 2017. MotionCor2: anisotropic correction of beam-induced motion for improved cryo-electron microscopy. Nat. Methods 14 (4), 331–332.

Zuo, F., et al., 2022. Heterologous immunization with inactivated vaccine followed by mRNA-booster elicits strong immunity against SARS-CoV-2 Omicron variant. Nat. Commun. 13 (1), 2670.